[CANCER RESEARCH 63, 5335–5343, September 1, 2003]

Atm-, p53-, and Gadd45a-Deficient Mice Show an Increased Frequency of Homologous Recombination at Different Stages during Development[1]

Alexander J. R. Bishop,[2] M. Christine Hollander, Bela Kosaras, Richard L. Sidman, Albert J. Fornace, Jr., and Robert H. Schiestl[3]

Department of Genetics and Howard Hughes Medical Institute, Harvard Medical School, Boston, Massachusetts 02115 [A. J. R. B.]; National Institutes of Health, National Cancer Institute, Bethesda, Maryland 20892 [M. C. H., A. F.]; Department of Neurology, Beth Israel Deaconess Medical Center, Harvard Institutes of Medicine, Boston, Massachusetts 02115 [B. K., R. L. S.]; and Department of Pathology, University of California at Los Angeles School of Medicine, Los Angeles, California 90095 [R. H. S.]

ABSTRACT

Atm, p53, and Gadd45a form part of a DNA-damage cellular response pathway; the absence of any one of these components results in increased genomic instability. We conducted an *in vivo* examination of the frequency of spontaneous homologous recombination in Atm-, p53-, or Gadd45a-deficient mice. In the absence of p53, we observed the greatest increase in events, a lesser increase in the absence of Atm, and only a modest increase in the absence of Gadd45a. The striking observation was the difference in the time at which the spontaneous events occurred in *atm* and *trp53* mutant mice. The frequency of homologous recombination in *atm* mutant mice was increased later during development. In contrast, p53 appears to have a role in suppressing homologous recombination early during development, when p53 is known to spontaneously promote p21 activity. The timing of the increased spontaneous recombination was similar in the Gadd45a- and p53-deficient mice. This temporal resolution suggests that Atm and p53 can act to maintain genomic integrity by different mechanisms in certain *in vivo* contexts.

INTRODUCTION

After cellular DNA damage, cells respond to and often repair the damage in an orchestrated manner. One signaling pathway that has been demonstrated to play a key role is the Trp53 (p53) damage response pathway (1–5). After the activation and stabilization of p53, p53 plays a central part in the type of responses that cells mount to a variety of damages. These responses include apoptosis, cell cycle arrest and DNA repair (reviewed in Ref. 6). It is now understood that p53 is normally maintained at a level within the cell that does not result in any significant transcriptional activation of its downstream effectors.

Atm is a protein kinase (7–9) that is activated in the cell after ionizing radiation exposure (10, 11). It is now clear that Atm has many targets (for a review see Ref. 12), among them is p53, which is effected both directly (2, 13–17) and indirectly (18–20). p53 can subsequently transcriptionally up-regulate effectors such as Cdkn1a (p21; see Ref. 21) and Gadd45a (2) to produce a coordinated cellular response. The up-regulation of p21 results in a cell cycle arrest at the G_1-S border (21–27), which is thought to allow time for repair reactions to be enacted. In what manner any repair reaction is controlled by p53 is not fully understood, although the absence of p53 or Gadd45a has been related to a decreased level of nucleotide excision repair (28). From the point of view of this report, it is interesting to note that the absence of the p53 damage response pathway components Atm (29–34), p53 (35, 36), or Gadd45a (37) has been observed to confer an increased level of genomic instability.

Our understanding of recombination is that there are a number of different types of recombination mechanisms, broadly divided into HR[4] and nonhomologous endjoining. HR is mediated by regions of homologous DNA and is the basis of the assay used in this study.

To determine the frequency of HR *in vivo*, we identified the number of cells or clones of cells that had deleted a 65-kb DNA duplication to a single copy (see Fig. 1). The duplication allele, called pink-eyed unstable (p^{un}; see Refs. 38, 39), interrupts the murine pigmentation gene, pink-eyed dilution (p). In the absence of a functional p gene, mice have pink eyes and a dilute coat color (40). Only a HR event will result in the correct reconstitution of the p gene and the phenotypic pigmentation that is assayed (38, 39). Molecular analysis has confirmed that these events are the result of p^{un} reversion (38, 39, 41). The p gene is normally transcribed in melanocytes and cells of the RPE, so that when a deletion/reversion event of p^{un} occurs somatically in a precursor of a melanocyte or RPE cell, this cell will proliferate and differentiate into a clone of pigmented cells. Such patches or spots have been observed in both the fur (38, 41) and eyes (42–44) of p^{un} mice. On the C57BL/6J inbred background, approximately 5–10% of p^{un} mice spontaneously display visible fur-spots (38, 41) and 4 to 5 eyes-pots are observed per RPE (44, 45).

Deletions reverting the p^{un} allele to p^{+} resulting in fur spots (fur-spot assay) are increased in frequency after exposure to different DNA-damaging agents (41, 46, 47), as well as in different cancer predisposing genetic backgrounds (34, 48). In those *in vivo* studies, *atm* mutant mice had an increased frequency of recombination (34), whereas the *trp53* mutant mice did not (49). This was surprising because a number of tissue culture studies with p53-deficient cells have demonstrated an increased frequency of recombination (50–54). To address this issue, we developed the p^{un} eye-spot assay. This assay has already proven to be more sensitive in detecting the frequency of recombination after exposure to DNA-damaging agents than the fur-spot assay (45). In addition, we demonstrated that because of the well-defined developmental pattern of the RPE (55), we were able to define the time at which a recombination event occurred by its position within the RPE (56). Here we use the p^{un} eye-spot assay to examine the frequency of spontaneous recombination in mice deficient for Atm, p53, or Gadd45a. The results demonstrated an increased frequency of HR in all three genetic backgrounds, but the timing of the instability was different between Atm-deficient and p53- or Gadd45a-deficient mice. This study confirms our earlier suggestion of an increased frequency of HR in *atm* mutant mice, while demonstrating that *trp53* and *gadd45a* mutant mice also display an increased frequency of HR early during development.

Received 12/18/02; revised 5/22/03; accepted 6/26/03.

The costs of publication of this article were defrayed in part by the payment of page charges. This article must therefore be hereby marked *advertisement* in accordance with 18 U.S.C. Section 1734 solely to indicate this fact.

[1] Supported by grants from the National Institute of Environmental Health Sciences, NIH, RO1 Grant ES09519 and KO2 Award ES00299 (to R. H. S.), NIH RCDA Award F32GM19147 (to A. J. R. B.), and an A-T Children's Fund award (to B. K. and R. L. S.).

[2] To whom requests for reprints should be addressed, at Department of Genetics, Harvard Medical School, 200 Longwood Avenue, Boston, MA 02115. Phone: (617) 432-7553; Fax: (617) 432-7663; E-mail: abishop@genetics.med.harvard.edu.

[3] To whom requests for reprints should be addressed, at Department of Pathology, UCLA School of Medicine, 650 Charles E. Young Drive South, Los Angeles, CA 90095. Phone: (310) 267-2087; Fax: (310) 267-2578; E-mail: rschiestl@mednet.ucla.edu.

[4] The abbreviations used are: HR, homologous recombination; RPE, retinal pigment epithelium; dpc, days post coitum.

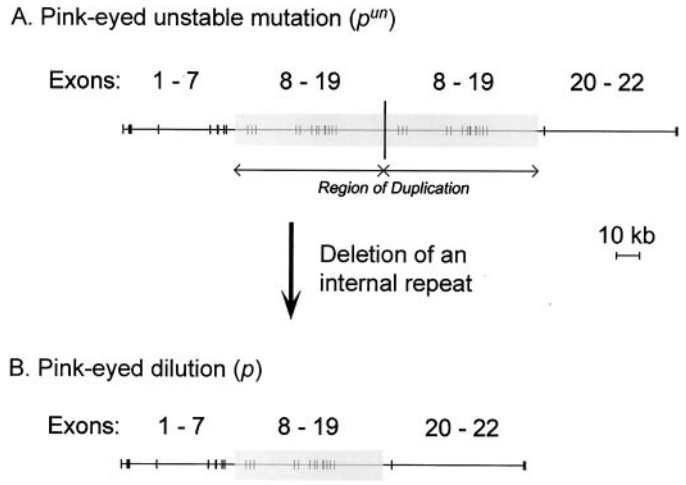

Fig. 1. A schematic representation of the pink-eyed unstable mutation (p^{un}; *A*) and the wild-type gene pink-eyed dilution (*p*; *B*). The publicly available murine sequences for the wild-type gene were obtained from the NIH (Internet address: www.ncbi.nlm.nih.gov/cgi-bin/Entrez/map_srchdb?chr = mouse_chr.inf). The duplication junction sequenced identified previously (39) were identified within the genomic region to generate the schematic. The duplication was found to include sequences from within intron 7 to within intron 19, spanning ~65 kb. The sequence representations are drawn to scale, a *10-kb scale bar* is given. The translation start is in exon 3 and, assuming correct splicing of all exons, the duplication will result in the insertion of a novel alanine created at the junction of exons 19 and 8, followed by 433 amino acids of the duplicated exons 8 to 19. After deletion of one of the internal repeats by HR, a functional protein can be produced and will result in pigmentation in either melanocytes or cells of the RPE.

MATERIALS AND METHODS

Mice. C57BL/6J- $p^{un/un}$ mice were obtained from the Jackson Laboratory (Bar Harbor, ME). C57BL/6J $p^{un/un}$ *Atm* $^{+/-}$ and C57BL/6J $p^{un/un}$ *Trp53*$^{+/-}$ have been described previously (34, 49). Mice heterozygous for *Atm* or *Trp53* and homozygous for p^{un} were bred to generate mice of all three *Atm* or *Trp53* genotypes. *Gadd45a* mutant mice (37) were bred into the C57BL/6J $p^{un/un}$ genetic background with three back-crosses to produce C57BL/6J-$p^{un/un}$ *Gadd45a*$^{-/-}$ mice that were maintained. In the generation of this colony, C57BL/6J-$p^{un/un}$ *Gadd45a*$^{+/+}$ mice were also produced and maintained as a control. All mice were bred in the institutional animal facility under standard conditions with a 12-h light/dark cycle and were fed standard diet and water *ad libitum*. The $p^{un/un}$ genotype was observed phenotypically in the progeny of the second back-cross as mice with a dilute (gray) coat color.

PCR Genotype. The *Atm*, *Trp53*, and *Gadd45* genotypes were determined by PCR amplification as described previously (34, 37, 49). DNA was prepared from tail biopsies by standard protocols.

Dissection of the RPE. Eyes from sacrificed 20-day-old mice were removed, fixed, and dissected to expose the RPE layer, as described previously (45, 55). The RPE adjacent to the neural retina was isolated for analysis by removing the eye from its orbit, immersing it in fixative [4% paraformaldehyde in 0.1 M phosphate buffer (pH 7.4)] for 1 h and then in PBS until dissection. An incision was made at the upper corneo-scleral border to allow removal of the cornea and lens. Six to eight incisions were made into the eyecup from the corneo-scleral margin toward the centrally positioned optic nerve. The dissected eyecup was placed on a glass slide with the retina facing up. The retina was then gently removed and the flattened eyecup, with RPE facing up, was mounted in 90% glycerol for analysis.

Scoring a Single-Reversion Event, Visualized As an Eye-Spot. We defined two or more adjacent pigmented cells, or pigmented cells separated from each other by no more than one unpigmented cell, as an eye-spot that resulted from one reversion event (55). The number of eye-spots in each RPE and the number of cells that comprised each eye-spot were counted. Positions of eye-spots were mapped.

Distance Analysis of Eye-Spots from the Optic Nerve. Spots were identified under the microscope and compared with their scanned digital images. Distances were measured with the Adobe PhotoShop 5.5 Measurement Tool. Distances were converted from pixels to millimeters by counting the number of pixels per millimeter on the image of a micron scale reticule scanned at the same optical settings as the RPE. Two distances were measured for each eye-spot: the "eye-spot distance," the distance from the center of the optic nerve head to the most proximal edge of the eye-spot; and the "RPE distance" of an eye-spot, the distance from the optic nerve through the eye-spot to the outer edge of the RPE. Dividing the eye-spot distance by the RPE distance gave the proportional distance of each eye-spot from the outer edge of the RPE, or its "position." The position of each eye-spot was determined in this manner to compensate for differences in the size of the eyes.

Microscope, Digital Camera, and Software. Whole-mount RPE were scanned by a DC120 digital camera (Eastman Kodak Company) mounted on a DMLB microscope (Leica Microsystems, Inc., Wetzlar, Germany) using a ×2.5 N-plan objective. Embryonic sections were scanned by a RT Slider Spot camera (Diagnostic Instruments, Inc., MI) mounted on a Axioskop microscope (Zeiss, Göttingen, Germany). The images were assembled and examined in Adobe PhotoShop 5.5 on a Macintosh Power Computer. All data were stored and processed with Microsoft Excel 2001.

Statistical Analysis. Comparison between numbers of events was performed by a standard *G* test (57). The *G* test is equivalent to a contingency χ^2 test, but allows for classes with zero events. Comparison of the population of events per RPE between genotypes was performed by Wilcoxon rank-sum analysis (58, 59).

RESULTS

Eye-Spot Frequency. An examination was conducted on the p^{un} reversion frequency in the RPE. The C57BL/6J- $p^{un/un}$ *Atm*$^{+/+}$, C57BL/6J- $p^{un/un}$ *Trp53*$^{+/+}$ and C57BL/6J- $p^{un/un}$ colonies described in previously reported concurrently performed studies (45, 56) were not maintained separately, and comparison of the wild-type retinal pigment epithelia revealed no significant difference in p^{un} reversion frequency or pattern (data not shown). The *Gadd45a* mouse colony was maintained separately; therefore, an extensive analysis was performed to compare the RPE of that colony with the rest of the wild-type controls. Of all of the analyses performed, a significant difference was only found by the relative positional distribution of events ($Z = 2.4$; $P_{(z)} \geq 0.015$). Taking this minor difference into account, we performed all further analyses for the *Gadd45a* colony separately from the other colonies and their wild-type controls.

The reversion frequency of the p^{un} locus was determined for 20 C57BL/6J- $p^{un/un}$ *Atm*$^{-/-}$, 16 C57BL/6J- $p^{un/un}$ *Trp53*$^{-/-}$, 40 C57BL/6J- $p^{un/un}$ combined wild-type control, 32 C57BL/6J- $p^{un/un}$ *Gadd45a*$^{-/-}$, and 26 C57BL/6J- $p^{un/un}$ *Gadd45a*$^{+/+}$ control RPE (see Table 1). One unexpected observation that came from this analysis was that 2 of the 16 RPE obtained from C57BL/6J- $p^{un/un}$ *Trp53*$^{-/-}$

Table 1 *Summary of eye-spot and pigmented cell frequency*

Genotype	Totals			Averages					
	RPE	Cells[a]	Spots	Cells[a] RPE	± SD	spots (*n*)	± SD	Spot Size[b]	± SD
Wildtype control	40	610	242	16.3	11.2	6.1	3.5	2.6	3.1
Gadd45a control	26	621	157	24.1	25.7	6.0	2.8	4.0	8.9
atm mutant	20	425	188	21.3	9.5	9.4	3.2	2.3	2.5
trp53 mutant	16	1265	255	79.1	145.4	15.9	17.4	5.0	7.0
gadd45a mutant	32	1260	283	39.4	150.6	8.8	13.8	4.5	7.8

[a] Pigmented cells.
[b] Spot size in number of pigmented cells.

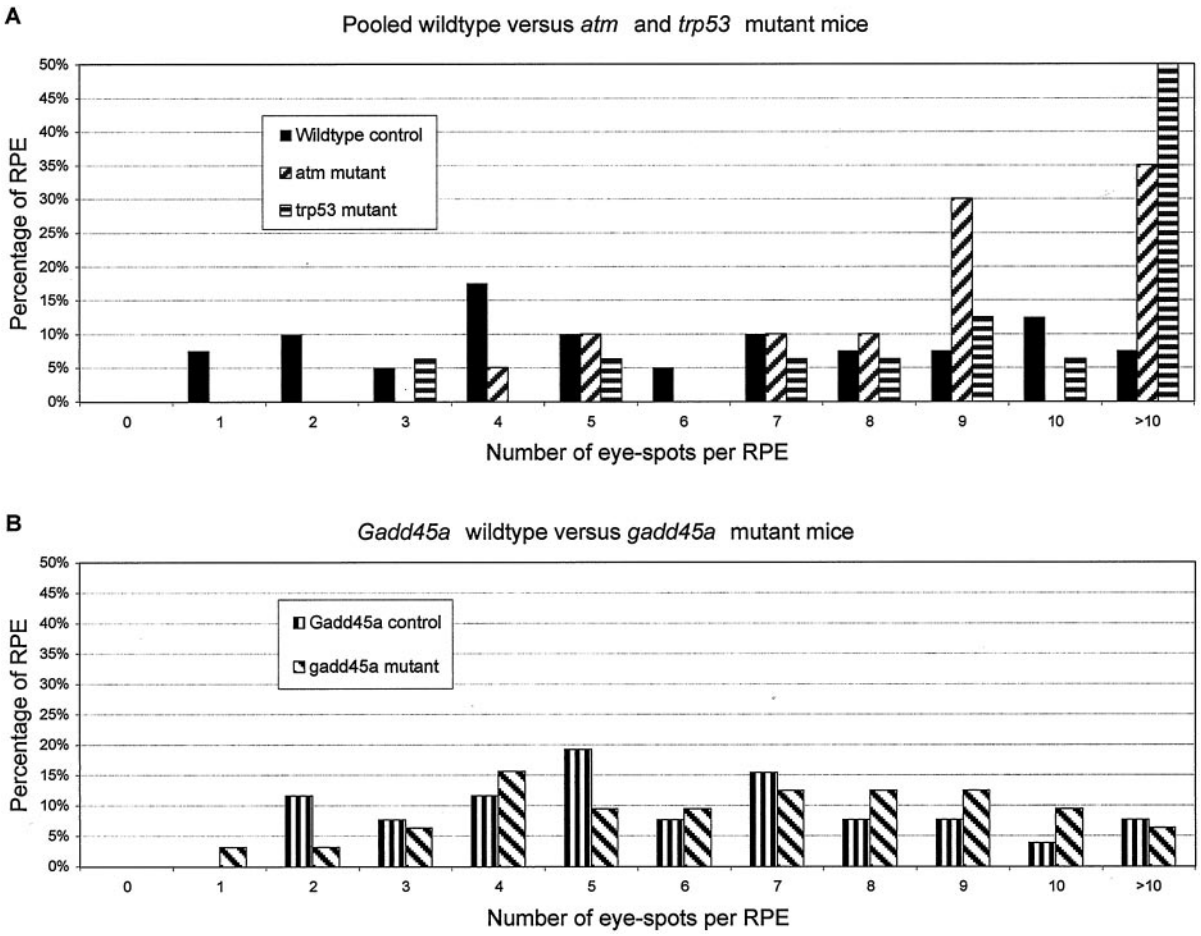

Fig. 2. Comparison of the number of eye-spots found per RPE in the each mutant genotype with their relevant control. *A*, a graphical representation of eye-spot frequency per RPE of *atm* and *trp53* mutant mice compared with the wild-type control. The majority of RPE obtained from the *atm* and *trp53* mutant mice have more than nine eye-spots, where the majority of wild-type control RPE have fewer than seven eye-spots. This difference is highly significant for both genotypes. *B*, a graphical representation of eye-spot frequency per RPE of *gadd45a* mutant mice compared with the *Gadd45a* control. There is no significant difference in the pattern of eye-spot frequency between these genotypes, although *Gadd45a* control RPE have six eye-spots on average whereas *gadd45a* mutant RPE have nine.

mice and 1 of 32 RPE obtained from C57BL/6J- $p^{un/un}$ $Gadd45a^{-/-}$ mice had what appeared to be a very early reversion events, possibly in progenitor RPE cells, resulting in many eye-spots. No such event has been observed in the 40 combined control RPE examined to date, nor the 26 C57BL/6J- $p^{un/un}$ $Gadd45a^{+/+}$, the additional 20 $Atm^{-/-}$ derived RPE reported here, or the 45 RPE obtained after either X-ray or benzo(*a*)pyrene exposure previously reported (45, 56). The frequency of such an early event in the $Trp53^{-/-}$ was significantly different from the combined control ($G = 5.199878$; $P_{(G)} \geq 0.023$), although the frequency observed for the $Gadd45a^{-/-}$ was not significantly different from the *Gadd45a* control ($G = 1.203654$; $P_{(G)} \geq 0.27$). The observation of these types of event is already indicative of an increased level of HR early in the development of the RPE in these genetic backgrounds.

The average number of reverted (pigmented) cells per RPE, eye-spots per RPE, and eye-spot size for all genotypes were determined (see Table 1). On average, all three mutant backgrounds had more reverted RPE cells and eye-spots compared with their controls, but only *trp53* and *gadd45a* mutant mice had an increased average eye-spot size. Because the SD in these analyses was similar to the average, a more correct method to examine the distribution of reversion frequency between the control and the mutant genotypes was to compare the distribution of RPE with a particular number of events, as shown graphically in Fig. 2. Performing a rank-sum analysis of these distributions demonstrated a significant difference between the pooled wild-type control and both *atm* and *trp53* mutant mice (see Fig. 2*A*; *atm* mutant mice: $Z = -3.2$; $P_{(Z)} \geq 0.0013$; *trp53* mutant mice: $Z = -3.6$; $P_{(Z)} \geq 0.0003$). The difference between *Gadd45a* wild-type and mutant mice was not significant (see Fig. 2*B*; *gadd45a* mutant mice: $Z = 0.9$; $P_{(Z)} \geq 0.37$). Therefore, after examining the overall frequency of spontaneous HR events, it was apparent that the *atm* and *trp53* mutant backgrounds displayed a greatly increased level of HR that was not observed in the *gadd45a* mutant background.

Examining the Frequency of Different Sized Eye-Spots. Eye-spots were categorized by size, that is, the number of reverted cells that constitute them. Previous reports have noted that the majority of eye-spots consisted of a single pigmented cell, with fewer two-cell eye-spots, even fewer three-cell eye-spots, and so on (44, 45, 56). We observed no difference in these ratios for either the *atm* mutant mice ($Z = 1.5$; $P_{(Z)} \geq 0.15$) or the *gadd45a* mutant mice ($Z = -0.2$; $P_{(Z)} \geq 0.85$) and their relevant controls (see Fig. 3, *B* and *D*, respectively). In contrast, *trp53* mutant mice had a significantly different eye-spot size distribution from both the pooled control ($Z = -4.1$; $P_{(Z)} \geq 4.2 \times 10^{-5}$) and even more so from the *atm* mutant mice ($Z = -5.1$; $P_{(Z)} \geq 3.3 \times 10^{-7}$). This size redistribution indicates that in the *trp53* mutant mice, more HR events occurred in cells that were likely to continue proliferating than was observed with either Atm-deficient or control mice. It is clear, however, that all three mutant backgrounds displayed an increased frequency of each sized eye-spot compared with their control (see Fig. 3, *A* and *C*).

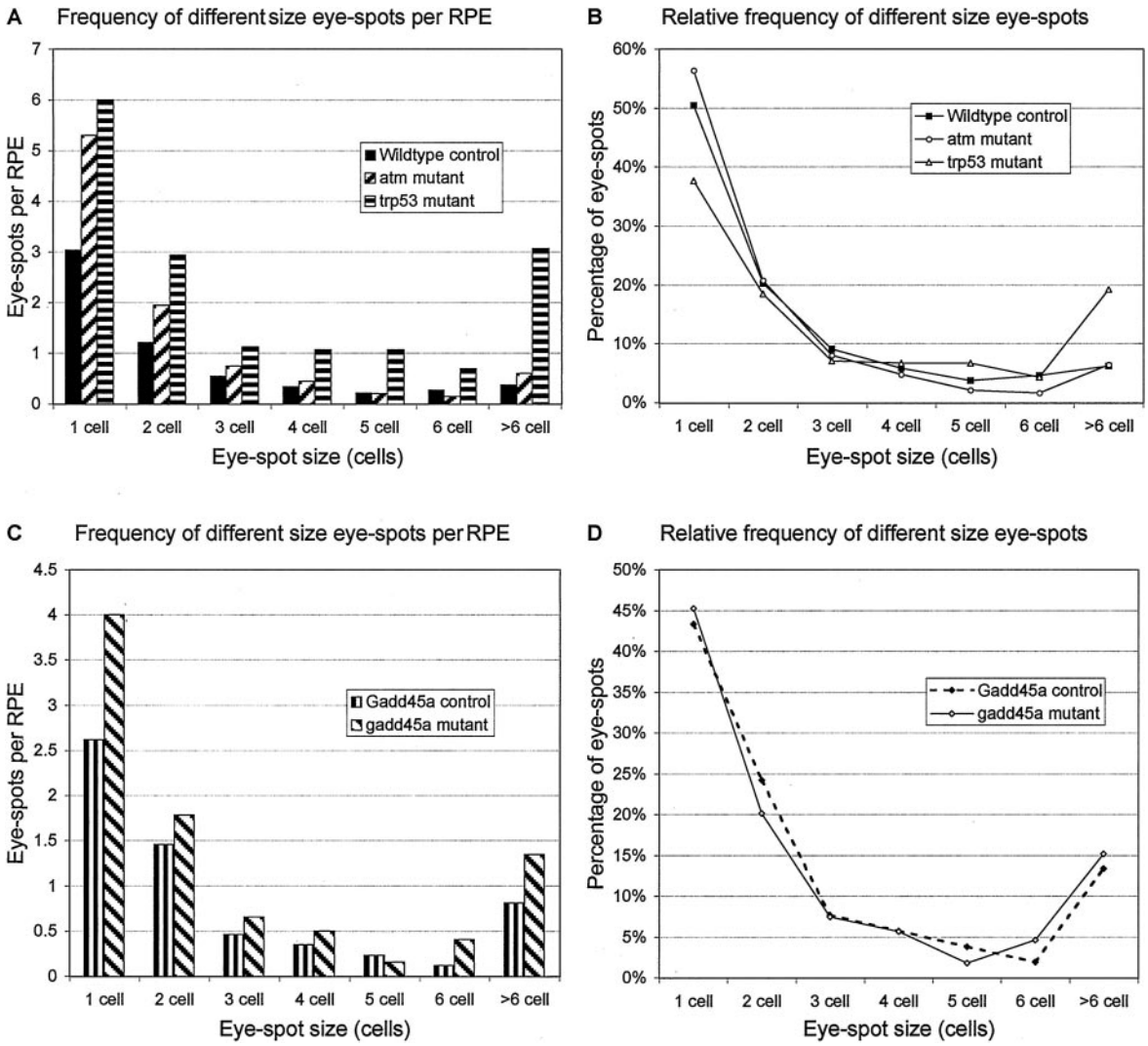

Fig. 3. Frequency and relative frequency of different size eye-spots in the RPE of the mutant mouse genotypes and their relevant controls. Eye-spot size is determined by the number of pigmented cells in the eye-spot. *A*, the frequency of different size eye-spots per RPE in *atm* and *trp53* mutant mice and the wild-type control. For all sizes of eye-spot, there is an increased frequency per RPE for both genotypes over the control. *B*, the relative frequency of each size eye-spot per RPE as a proportion of all of the other eye-spots found in *atm* and *trp53* mutant mice and the wild-type control. In both the control wild-type and *atm* mutant RPE >50% of the eye-spots consisted of only a single cell. Although *trp53* mutant RPE also displayed a majority of singlet eye-spots, there were proportionally more larger eye-spots. *C*, the frequency of different size eye-spots per RPE in *gadd45a* mutant mice and the *Gadd45a* control. The *gadd45a* mutant RPE had more of each size eye-spot per RPE than the control. *D*, the relative frequency of each size eye-spot per RPE as a proportion of all of the other eye-spots found in *gadd45a* mutant mice and the *Gadd45a* control. The distribution of the eye-spot sizes appear to be the same between this mutant genotype and its control.

Examining the Positional Distribution of Eye-Spots in the RPE. We examined the frequency of eye-spots located in different position intervals for the different mutant backgrounds and their relevant controls (see Figs. 4*A* and 5*A*). The data obtained are displayed either as a frequency per RPE over positional intervals or as a relative frequency distribution that more clearly illustrates the pattern of recombination frequency by position. To determine whether there was any significant difference between the positional distributions of these eye-spots in different genotypes, rank-sum analyses were performed. Because we determined previously that the pattern of eye-spots can be resolved into two populations, eye-spots consisting of a single pigmented cell (singlets) and larger eye-spots (56), with distinguishable distribution patterns, larger eye-spots generally lying more distal to the optic nerve head than the singlets (56), any positional analysis benefits from the individual consideration of each type of eye-spot population. The distributions of singlet (see Figs. 4*B* and 5B) and larger eye-spots (see Figs. 4*C* and 5*C*) are also given.

The *atm* mutant mice had an ~30% increase in the frequency of events compared with the wild-type control for each position examined (see Fig. 4*A*). The greatest increase in frequency of events was found in the singlet eye-spot class, as compared with the control (compare eye-spot frequency for *atm* mutant mice in Fig. 4, *C* and *E*). The most interesting aspect of these results, however, is that the overall distribution of these HR events was the same as the distribution found in the wild-type control (Fig. 4*B*; $Z = 0.4$; $P_{(Z)} \geq 0.66$). The same was found to be true with both the singlet (Fig. 4, *C* and *D*; $Z = -0.2$; $P_{(Z)} \geq 0.86$) and larger (Fig. 4, *E* and *F*; $Z = 0.7$; $P_{(Z)} \geq 0.48$) eye-spot populations. These results suggest that although there is an increased amount of HR in the *atm* mutant mouse, the timing and types of event is directly comparable with the pattern observed for wild-type mice.

The *trp53* mutant mice had an increased frequency of events at all positions compared with the wild-type control, irrespective of whether examining all eye-spots, the singlets or the larger eye-spots (see Fig. 4, *A*, *C*, and *E*, respectively). The largest increase in events was observed in the optical nerve head proximal region, leading to a significant redistribution in the relative positional pattern of HR events (all eye-spots, Fig. 4*B*: $Z = 6.0$, $P_{(Z)} \geq 2.4 \times 10^{-9}$; singlets,

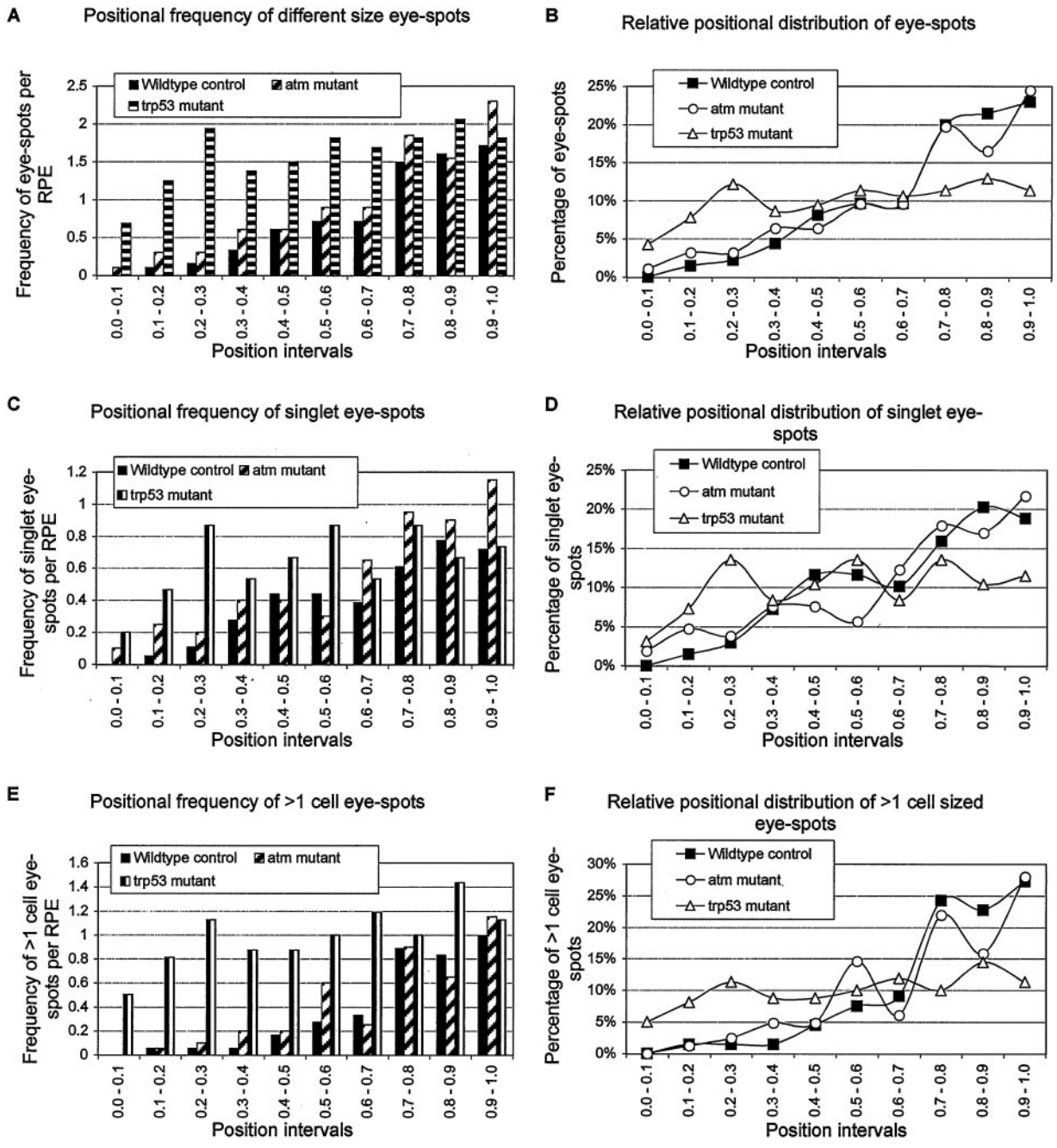

Fig. 4. An examination of the frequency of eye-spots in different regions of the RPE of *atm* and *trp53* mutant mice compared with the wild-type mice. Results are presented as either the absolute frequency per RPE (*A*, *C*, and *E*) or as a relative positional distribution (*B*, *D*, and *F*). A *position* of *0.0* is equivalent to the optic nerve head, whereas a *position* of *1.0* is at the edge of the RPE. Examination was conducted on all sized eye-spots combined (*A* and *B*), singlet eye-spots (*C* and *D*), or only the larger eye-spots (*E* and *F*). Examination of the absolute frequency of events for the 20 *atm* mutant and 18 of the wild-type RPE (*A*, *C*, and *E*) demonstrates that the frequency of eye-spots of all classes increase from the optic nerve to the periphery of the RPE. This is represented in the positional distributions (*B*, *D*, and *F*) by the increasing proportion of events from 0% at *positions 0.0–0.1* to 25% at *positions 0.9–1.0*, the edge of the RPE. The eye-spot distribution in the RPE derived from the 16 *trp53* mutant mice do not display this gradient effect, with the most obvious difference seen with the larger eye-spots (*E* and *F*).

Fig. 4*D*: $Z = 3.1$, $P_{(Z)} \geq 0.0017$; larger eye-spots, Fig. 4*F*: $Z = 5.4$, $P_{(Z)} \geq 7.6 \times 10^{-8}$), most dramatically in the larger eye-spot population. The distributions of eye-spots in the *atm* and *trp53* mutant mice were also compared and gave similar results, demonstrating a significant difference in the pattern of events for these two genotypes (all eye-spots, Fig. 4*B*: $Z = 5.9$, $P_{(Z)} \geq 4.8 \times 10^{-9}$; singlets, Fig. 4D: $Z = 3.5$, $P_{(Z)} \geq 0.00050$; larger eye-spots, Fig. 4*F*: $Z = 4.9$, $P_{(Z)} \geq 8.8 \times 10^{-7}$).

The positional distribution of events in the *gadd45a* mutant was compared with the *Gadd45a* control. An overall increased frequency of events was observed for most positions (Fig. 5*A*), although this increase seemed to be mostly attributable to the increase in larger eye-spots (compare Fig. 5, *C* and *E*). Similar to the results with the *trp53* mutant mice, the greatest increase in events were found proximal to the optic nerve head, although a significant difference was only found for the total events and more so for the larger eye-spots compared with the control distribution (all eye-spots, Fig. 5*B*: $Z = 2.8$, $P_{(Z)} \geq 0.0052$; singlets, Fig. 5*D*: $Z = 0.7$, $P_{(Z)} \geq 0.47$; larger eye-spots, Fig. 5*F*: $Z = 3.2$, $P_{(Z)} \geq 0.0016$).

An alternative method to examining the overall frequency dis-

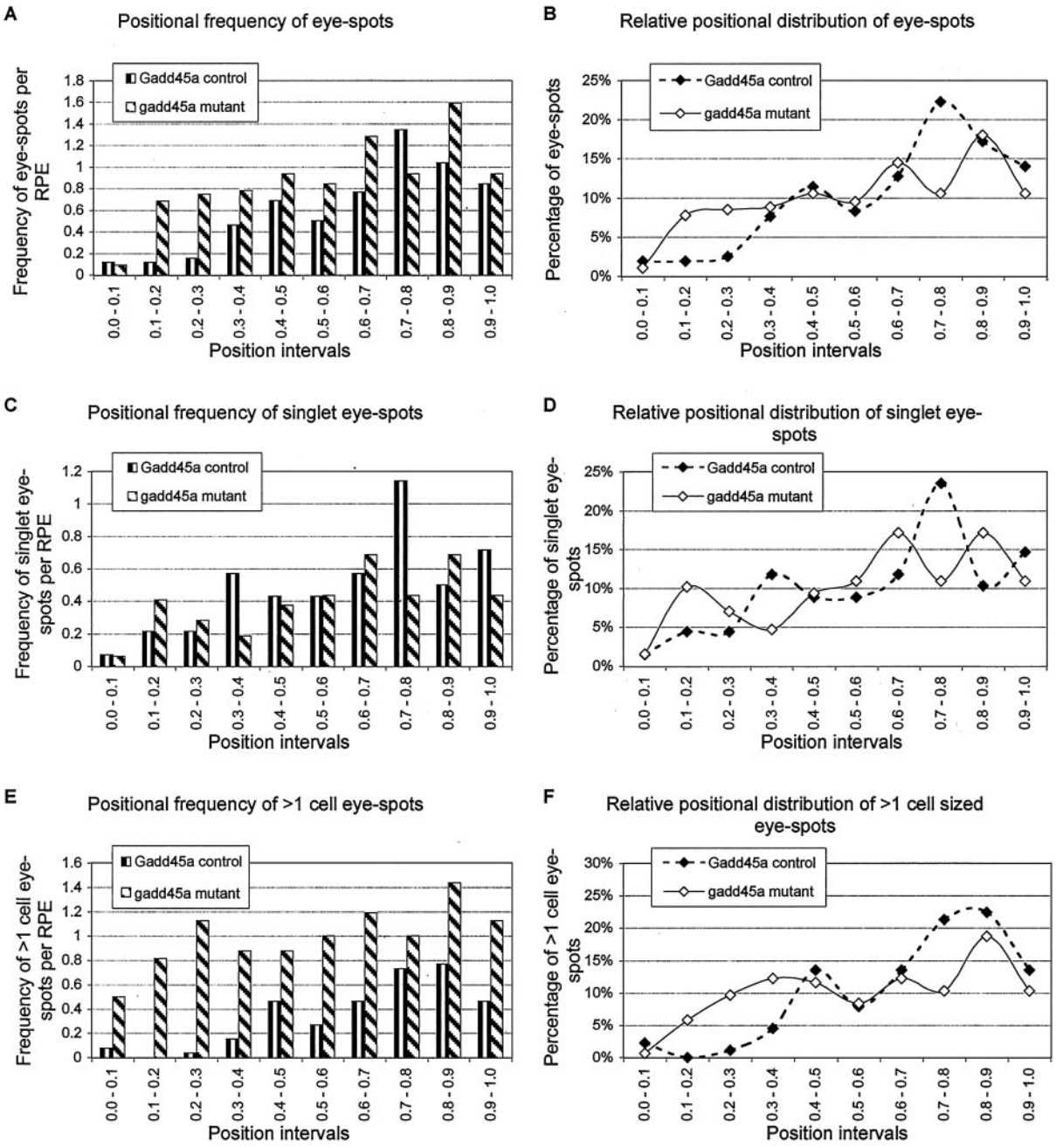

Fig. 5. An examination of the frequency of eye-spots in different regions of the RPE of *gadd45a* mutant mice compared with the *Gadd45a* control mice. Results are presented as either the absolute frequency per RPE (*A*, *C*, and *E*) or as a relative positional distribution (*B*, *D*, and *F*). A *position* of *0.0* is equivalent to the optic nerve head, whereas a *position* of *1.0* is at the edge of the RPE. Examination was conducted on all sized eye-spots combined (*A* and *B*), singlet eye-spots (*C* and *D*) or only the larger eye-spots (*E* and *F*). The distribution of eye-spots in the 32 *gadd45a* mutant RPE examined is significantly different from the eye-spot distribution of the 26 control RPE. The most significant difference between *gadd45a* mutant and the control eye-spot distribution can be observed for the larger eye-spots (*E* and *F*), with an increased proportion of eye-spots located proximal to the optic nerve in the mutant background.

tribution of eye-spots is to compare the frequency of events within a defined region *versus* the frequency of events outside of that region. Previously, we have used this method to identify specific regions into which there has been a redistribution of recombination events compared with control (56). The results of these analyses are given in Table 2 and correlate very well with the rank-sum analyses performed on the overall eye-spot distribution patterns (compare Table 2 regions with Fig. 4, *B*, *D*, and *F*, and Fig. 5, *B*, *D*, and *F*). Comparison between the *atm* mutant mice and the wild-type control revealed no region of significant difference and was, therefore, not included. *Trp53* mutant mice demonstrated regions of significant increase and a corresponding region of decrease, compared with the pooled wild-type control for every class of eye-spot. *Gadd45a* mutant mice demonstrated a very similar pattern to the *trp53* mutant mice with the exception that no region of significantly increased singlet eye-spots was identified, only a region of decrease distal to the optic nerve head. These results strongly suggest that the profile of events found in the *trp53* and *gadd45a* mutant backgrounds are very similar, and yet both are very different from the profiles observed for the *atm* mutant mice. In addition, examining either the total population distribution or limiting the analysis to specific regions demonstrates that the greatest effect of *trp53* and *gadd45a* mutations is an increased frequency of larger eye-spots. Region analysis locates these events

Table 2 *Comparing the frequencies of eye-spots of different classes in specific regions between mutant and control genotypes*

		Mutant frequency				Control frequency				Statistics	
Mutation	Region[a]	In[b]	Rest[c]	Total[d]	Percentage in[b]	In	Rest	Total	Percentage in	*G*	*P*
All eye-spots											
trp53 mutant	0.7–1.0	91	164	255	36%	87	48	135	64%	29.7	5.16×10^{-8}
trp53 mutant	0.0–0.4	84	171	255	33%	11	124	135	8%	33.6	6.83×10^{-9}
gadd45a mutant	0.7–0.8	30	253	283	11%	35	122	157	22%	10.5	1.17×10^{-3}
gadd45a mutant	0.0–0.3	46	237	283	16%	7	150	157	4%	15.2	9.49×10^{-5}
Singlet eye-spots											
trp53 mutant	0.7–1.0	34	62	96	35%	38	31	69	55%	6.3	1.20×10^{-2}
trp53 mutant	0.0–0.3	23	73	96	24%	3	66	69	4%	13.4	2.57×10^{-4}
gadd45a mutant	0.7–0.8	14	114	128	11%	16	52	68	24%	5.2	2.26×10^{-2}
>1-cell eye-spots											
trp53 mutant	0.7–1.0	57	102	159	36%	49	17	66	74%	28.3	1.01×10^{-7}
trp53 mutant	0.0–0.5	67	92	159	42%	6	60	66	9%	26.9	2.15×10^{-7}
gadd45a mutant	0.7–1.0	61	94	155	39%	51	38	89	57%	7.3	6.73×10^{-3}
gadd45a mutant	0.0–0.4	43	112	155	28%	5	84	89	6%	20.4	6.28×10^{-6}

[a] Region of RPE selected for comparison.
[b] Number of eye-spots in region selected.
[c] Number of eye-spots not in selected region.
[d] Total number of eye-spots.

proximal to the optic nerve head. Together, these observations suggest that there is an increased frequency of HR events initiated early during development in the *trp53* and *gadd45a* mutant mice, where the *atm* mutant mice have an increased frequency of events later in development in a pattern that recapitulates the pattern observed for wild-type mice.

DISCUSSION

The goal of this study was to examine the roles of Atm, p53, and Gadd45a in controlling the frequency of HR *in vivo*. Using a similar *in vivo* system (the p^{un} fur-spot assay), we previously reported that *atm* mutant mice have an increased frequency of HR and suggested that this increase came later during development (34). The increased level of recombination may not have been surprising, considering that cells from AT patients display a higher than normal frequency of genomic instability, but the timing aspect was unexpected. In addition, we also reported previously the spontaneous effect of *trp53* deficiency on the p^{un} fur-spot assay (49). In that study, we had the surprising finding that there was no observable increase in spontaneous HR frequency. Since that time, we developed and characterized the p^{un} eye-spot assay (45). With this assay, we defined a relationship between the regions in the adult mouse RPE where an increased level of HR occurred at the time of exposure to an HR-inducing agent during development and the region of proliferation of the RPE at that time of development (56). Thus, the p^{un} eye-spot assay provides both a more sensitive assay to determine the frequency of HR events *in vivo* and the ability to understand the timing of such events during development. With these tools, we have reexamined the roles of Atm and p53 in controlling the level of spontaneous HR during the development of the mouse embryo. In addition, we have included the *gadd45a* mutant mouse.

The study presented here clearly demonstrates that *atm* and *trp53* mutant mice have an increased frequency of spontaneous HR events compared with control mice. In addition, we have observed that the *gadd45a* mutant mice also have an increased frequency of HR, although only observable at a significant level by the positional distribution of events in the RPE. The striking result is that the profile of events in the *atm* mutant background is clearly different from the profile observed in the *trp53* and *gadd45a* mutant backgrounds, which are very similar to each other. In particular, the major spontaneous effect of the *trp53* and *gadd45* mutant backgrounds appears to be early in development, whereas the *atm* mutant background seems to affect spontaneous HR at later times of development, increasing at the same rate as wild-type spontaneous events.

The RPE of the mouse is a monolayer of pigmented cells derived from the neural epithelium. The development of this tissue in the mouse follows a well-defined pattern. RPE precursors enter the embryonic eyecup around the optic nerve head at about 8.5 dpc (60); the RPE then develops radially away from the optic nerve, with an outer edge-biased pattern of proliferation (55). In a previous study, we examined with the p^{un} eye-spot assay the effect of exposure to recombination-inducing agents at different times during development (56). We demonstrated that because of the well-defined developmental pattern of the RPE (55), we were able to define the time at which a recombination event occurred by its position within the RPE (56). The earliest exposure was at 8.5 dpc and resulted in a significant increase in events in almost the exact same position as observed here for the *trp53* and *gadd45a* mutant mice, if not slightly more distal from the optic nerve head. These results would suggest that the both *trp53* and *gadd45a* are playing a role in maintaining genomic stability early during development, before 8 dpc.

In our previous report on the effect of *trp53* on spontaneous HR frequency using the p^{un} fur-spot assay, we observed no difference in the frequency of events compared with wild-type control (49). In our efforts over the last decade to characterize the p^{un} fur-spot assay for the most responsive time during development to conduct an exposure to a DNA-damaging agent to demonstrate induction of HR, we found that exposure on 10.5 dpc had the best result. Exposure at 8.5 dpc resulted in little induction, presumably because of the low number of target melanoblasts, whereas exposure at 12.5 dpc resulted in fur-spots that were extremely difficult to detect, probably because of the number of cell divisions left was too limited to make an easily recognizable pigmented spot (data not shown). This would suggest that the p^{un} fur-spot assay would be insensitive to genomic instability at or before 8.5 dpc. Because we suggest that the time before 8 dpc is when an increased level of HR is seen in the *trp53* mutant mice, our previous study would have missed that effect.

There have been three reports in the literature on the spontaneous activity of p53 during mouse embryonic development (61–63), that is, the p53 dependent transcriptional activation of its downstream effector p21. All three studies reported that p53 is spontaneously active in the embryo up to approximately 8 dpc, when, depending on the tissue and level of differentiation, the spontaneous activity ceases. The lack of spontaneous activity later in development does not preclude the inducibility of p53 after exposure to DNA-damaging agents. These

reports have been substantiated by the early embryonic lethality of Mdm2-deficient mice and their rescue by a p53-null genetic background (64, 65), suggesting that p53 is highly active over this period and must be negatively regulated. In addition, the hypersensitivity of embryos to ionizing radiation over this same period (66, 67), before 8 dpc, also suggests an already potentiated damage response system that is easily triggered to promote an apoptotic response.

The timing of the increased HR frequency in the absence of p53 that we report here correlates surprisingly well with the spontaneous activity of p53 during embryonic development. The majority of events in the *trp53* and *gadd45a* mutant backgrounds appear to occur early, which, as a consequence, results in not only an increased number of events, but also an increase in larger eye-spots compared with singlets. These observations suggest a role for p53 and Gadd45a in maintaining genomic stability early in the developing embryo, similar to that seen in proliferating tissue culture studies (50–54). In addition, the results presented here strongly suggest that p53 and Gadd45a are acting in a similar fashion to control spontaneous HR, perhaps acting epistatically, as has already been established by the transcriptional regulation of Gadd45a by p53 in response to exogenous exposure to DNA-damaging agents (2). Considering that nucleotide excision repair is compromised in the p53 and Gadd45a-deficient backgrounds (28), it is possible that the HR machinery, in the absence of p53 or Gadd45a, has more opportunity to act on lesions that are normally repaired by nucleotide-excision repair. The result would be the observed increase in HR frequency in these mutant backgrounds. When p53 or Gadd45a are not spontaneously active, we would not expect to see a substantial increase in HR frequency above the background, correspondingly, the fold increase of HR over control is less later in development as determined by the eye-spot assay.

The results from the *atm* mutant mice directly correlates with our previous findings with the p^{un} fur-spot assay, an increased frequency of spontaneous recombination that increases more in later embryonic development. In addition, the majority of events, leading to greatest increase, were observed in the singlet eye-spots, unlike the observed profile of the *trp53* and *gadd45* mutant mice, where the greatest increase was in the frequency of larger eye-spots. This suggests that the role of Atm is very different from p53 in regulating spontaneous HR during development.

In the last few years, it has been demonstrated that Atm is involved in adult neurogenesis (68). To address the possibility that the observed HR patterning was attributable to a defect in RPE proliferation or development we examined the proliferation of RPE cells in 12.5 dpc embryos by BrdUrd incorporation (data not shown). Although markedly smaller and, in fact, 1-day developmentally delayed, determined by the lack of postmitotic ganglion cells, the RPE of *atm* mutant mice displayed no gross abnormality or any mispatterning of proliferation. We would, therefore, suggest that Atm does not have a tissue-specific role in RPE differentiation or development and is unlikely to be affecting the HR pattern in the RPE by perturbing its genesis.

In summary, we have demonstrated that p53 and Gadd45a play a role in suppressing HR during *in vivo* development similar to reports from tissue-culture studies. Unlike the tissue-culture studies, we have seen, both directly in this study and indirectly in our previous study (49), that this effect does not play a role later during the development of the embryo in either a neural epithelial or a neural crest derived tissue. This points to the necessity of relating tissue-culture studies on genomic stability with an *in vivo* model. In addition, this study also raises the question of the function of p53 and Gadd45a later in embryo development and how this function changes. Finally, we clearly demonstrate that Atm is functioning very differently from p53 and Gadd45a in suppressing HR, acting later in development. This synergy is supported by the increased prenatal death, severe runting, and increased rate of lymphoma reported in the generation of *atm trp53* double-mutant mice (69). Both Atm and p53 act as guardians for genomic stability, yet the differences in their time of action may offer some explanation as to the timing of carcinogenesis in these mouse models, with Atm-deficient mice suffering a more rapid rate of lymphoma onset (32, 33, 70) than p53-deficient mice (71, 72). If the level of HR stays abnormally high level in Atm-deficient mice, there is a great likelihood that HR events might directly cause oncogenic mutations or might more rapidly result in exposure of mutations in tumor suppressors. In p53-deficient mice, if the initial high burst of HR during development does not have a deleterious effect, the absence of p53 may have an effect later in the life when a cell is presented with a genomic insult and, in the absence of p53, will not be able to suppress an inappropriate HR event.

REFERENCES

1. Kastan, M. B., Onyekwere, O., Sidransky, D., Vogelstein, B., and Craig, R. W. Participation of p53 protein in the cellular response to DNA damage. Cancer Res., *51:* 6304–6311, 1991.
2. Kastan, M. B., Zhan, Q., el-Deiry, W. S., Carrier, F., Jacks, T., Walsh, W. V., Plunkett, B. S., Vogelstein, B., and Fornace, A. J., Jr. A mammalian cell cycle checkpoint pathway utilizing p53 and GADD45 is defective in ataxia-telangiectasia. Cell, *71:* 587–597, 1992.
3. Lu, X., and Lane, D. P. Differential induction of transcriptionally active p53 following UV or ionizing radiation: defects in chromosome instability syndromes? Cell, *75:* 765–778, 1993.
4. Zhan, Q., Carrier, F., and Fornace, A. J., Jr. Induction of cellular p53 activity by DNA-damaging agents and growth arrest (Published erratum in Mol. Cell. Biol. *13:* 5928, 1993). Mol. Cell. Biol., *13:* 4242–4250, 1993.
5. Hupp, T. R., Sparks, A., and Lane, D. P. Small peptides activate the latent sequence-specific DNA binding function of p53. Cell, *83:* 237–245, 1995.
6. Bargonetti, J., and Manfredi, J. J. Multiple roles of the tumor suppressor p53. Curr. Opin. Oncol., *14:* 86–91, 2002.
7. Keegan, K. S., Holtzman, D. A., Plug, A. W., Christenson, E. R., Brainerd, E. E., Flaggs, G., Bentley, N. J., Taylor, E. M., Meyn, M. S., Moss, S. B., Carr, A. M., Ashley, T., and Hoekstra, M. F. The Atr and Atm protein kinases associate with different sites along meiotically pairing chromosomes. Genes Dev., *10:* 2423–2437, 1996.
8. Chen, G., and Lee, E. The product of the *ATM* gene is a 370-kDa nuclear phosphoprotein. J. Biol. Chem., *271:* 33693–33697, 1996.
9. Jung, M., Kondratyev, A., Lee, S. A., Dimtchev, A., and Dritschilo, A. *ATM* gene product phosphorylates I κ B-α. Cancer Res., *57:* 24–27, 1997.
10. Shieh, S. Y., Ikeda, M., Taya, Y., and Prives, C. DNA damage-induced phosphorylation of p53 alleviates inhibition by MDM2. Cell, *91:* 325–334, 1997.
11. Siliciano, J. D., Canman, C. E., Taya, Y., Sakaguchi, K., Appella, E., and Kastan, M. B. DNA damage induces phosphorylation of the amino terminus of p53. Genes Dev., *11:* 3471–3481, 1997.
12. Shiloh, Y. ATM (ataxia telangiectasia mutated): expanding roles in the DNA damage response and cellular homeostasis. Biochem. Soc. Trans., *29:* 661–666, 2001.
13. Khanna, K. K., and Lavin, M. F. Ionizing radiation and UV induction of p53 protein by different pathways in ataxia-telangiectasia cells. Oncogene, *8:* 3307–3312, 1993.
14. Canman, C. E., Wolff, A. C., Chen, C. Y., Fornace, A. J., Jr., and Kastan, M. B. The p53-dependent G_1 cell cycle checkpoint pathway and ataxia- telangiectasia. Cancer Res., *54:* 5054–5058, 1994.
15. Savitsky, K., Bar-Shira, A., Gilad, S., Rotman, G., Ziv, Y., Vanagaite, L., Tagle, D. A., Smith, S., Uziel, T., Sfez, S., *et al*. A single ataxia telangiectasia gene with a product similar to PI-3 kinase. Science (Wash. DC), *268:* 1749–1753, 1995.
16. Barlow, C., Brown, K. D., Deng, C. X., Tagle, D. A., and Wynshaw-Boris, A. Atm selectively regulates distinct p53-dependent cell-cycle checkpoint and apoptotic pathways. Nat. Genet., *17:* 453–456, 1997.
17. Banin, S., Moyal, L., Shieh, S., Taya, Y., Anderson, C. W., Chessa, L., Smorodinsky, N. I., Prives, C., Reiss, Y., Shiloh, Y., and Ziv, Y. Enhanced phosphorylation of p53 by ATM in response to DNA damage. Science (Wash. DC), *281:* 1674–1677, 1998.
18. Khosravi, R., Maya, R., Gottlieb, T., Oren, M., Shiloh, Y., and Shkedy, D. Rapid ATM-dependent phosphorylation of MDM2 precedes p53 accumulation in response to DNA damage. Proc. Natl. Acad. Sci. USA, *96:* 14973–14977, 1999.
19. de Toledo, S. M., Azzam, E. I., Dahlberg, W. K., Gooding, T. B., and Little, J. B. ATM complexes with HDM2 and promotes its rapid phosphorylation in a p53-independent manner in normal and tumor human cells exposed to ionizing radiation. Oncogene, *19:* 6185–6193, 2000.
20. Maya, R., Balass, M., Kim, S. T., Shkedy, D., Leal, J. F., Shifman, O., Moas, M., Buschmann, T., Ronai, Z., Shiloh, Y., Kastan, M. B., Katzir, E., and Oren, M. ATM-dependent phosphorylation of Mdm2 on serine 395: role in p53 activation by DNA damage. Genes Dev., *15:* 1067–1077, 2001.
21. el-Deiry, W. S., Tokino, T., Velculescu, V. E., Levy, D. B., Parsons, R., Trent, J. M., Lin, D., Mercer, W. E., Kinzler, K. W., and Vogelstein, B. WAF1, a potential mediator of p53 tumor suppression. Cell, *75:* 817–825, 1993.
22. Xiong, Y., Hannon, G. J., Zhang, H., Casso, D., Kobayashi, R., and Beach, D. p21 is a universal inhibitor of cyclin kinases. Nature (Lond.), *366:* 701–704, 1993.

23. Harper, J. W., Adami, G. R., Wei, N., Keyomarsi, K., and Elledge, S. J. The p21 Cdk-interacting protein Cip1 is a potent inhibitor of G_1 cyclin- dependent kinases. Cell, *75:* 805–816, 1993.
24. Dulic, V., Kaufmann, W. K., Wilson, S. J., Tlsty, T. D., Lees, E., Harper, J. W., Elledge, S. J., and Reed, S. I. p53-dependent inhibition of cyclin-dependent kinase activities in human fibroblasts during radiation-induced G_1 arrest. Cell, *76:* 1013–1023, 1994.
25. Di Leonardo, A., Linke, S. P., Clarkin, K., and Wahl, G. M. DNA damage triggers a prolonged p53-dependent G_1 arrest and long-term induction of Cip1 in normal human fibroblasts. Genes Dev., *8:* 2540–2551, 1994.
26. Deng, C., Zhang, P., Harper, J. W., Elledge, S. J., and Leder, P. Mice lacking p21CIP1/WAF1 undergo normal development, but are defective in G_1 checkpoint control. Cell, *82:* 675–684, 1995.
27. Gu, W., and Roeder, R. G. Activation of p53 sequence-specific DNA binding by acetylation of the p53 C-terminal domain. Cell, *90:* 595–606, 1997.
28. Smith, M. L., Ford, J. M., Hollander, M. C., Bortnick, R. A., Amundson, S. A., Seo, Y. R., Deng, C. X., Hanawalt, P. C., and Fornace, A. J., Jr. p53-mediated DNA repair responses to UV radiation: studies of mouse cells lacking *p53*, *p21*, and/or *gadd45* genes. Mol. Cell. Biol., *20:* 3705–3714, 2000.
29. Bigbee, W. L., Langlois, R. G., Swift, M., and Jensen, R. H. Evidence for an elevated frequency of *in vivo* somatic cell mutations in ataxia telangiectasia. Am. J. Hum. Genet., *44:* 402–408, 1989.
30. Kojis, T. L., Gatti, R. A., and Sparkes, R. S. The cytogenetics of ataxia telangiectasia. Cancer Genet. Cytogenet., *56:* 143–156, 1991.
31. Meyn, M. S. High spontaneous intrachromosomal recombination rates in ataxia-telangiectasia. Science (Wash. DC), *260:* 1327–1330, 1993.
32. Barlow, C., Hirotsune, S., Paylor, R., Liyanage, M., Eckhaus, M., Collins, F., Shiloh, Y., Crawley, J. N., Ried, T., Tagle, D., and Wynshaw-Boris, A. Atm-deficient mice: a paradigm of ataxia telangiectasia. Cell, *86:* 159–171, 1996.
33. Elson, A., Wang, Y., Daugherty, C. J., Morton, C. C., Zhou, F., Campos-Torres, J., and Leder, P. Pleiotropic defects in ataxia-telangiectasia protein-deficient mice. Proc. Natl. Acad. Sci. USA, *93:* 13084–13089, 1996.
34. Bishop, A. J., Barlow, C., Wynshaw-Boris, A. J., and Schiestl, R. H. Atm deficiency causes an increased frequency of intrachromosomal homologous recombination in mice. Cancer Res., *60:* 395–399, 2000.
35. Purdie, C. A., Harrison, D. J., Peter, A., Dobbie, L., White, S., Howie, S. E., Salter, D. M., Bird, C. C., Wyllie, A. H., Hooper, M. L., *et al*. Tumour incidence, spectrum and ploidy in mice with a large deletion in the *p53* gene. Oncogene, *9:* 603–609, 1994.
36. Donehower, L. A., Godley, L. A., Aldaz, C. M., Pyle, R., Shi, Y. P., Pinkel, D., Gray, J., Bradley, A., Medina, D., and Varmus, H. E. Deficiency of p53 accelerates mammary tumorigenesis in Wnt-1 transgenic mice and promotes chromosomal instability. Genes Dev., *9:* 882–895, 1995.
37. Hollander, M. C., Sheikh, M. S., Bulavin, D. V., Lundgren, K., Augeri-Henmueller, L., Shehee, R., Molinaro, T. A., Kim, K. E., Tolosa, E., Ashwell, J. D., Rosenberg, M. P., Zhan, Q., Fernandez-Salguero, P. M., Morgan, W. F., Deng, C. X., and Fornace, A. J., Jr. Genomic instability in Gadd45a-deficient mice. Nat. Genet., *23:* 176–184, 1999.
38. Brilliant, M. H., Gondo, Y., and Eicher, E. M. Direct molecular identification of the mouse pink-eyed unstable mutation by genome scanning. Science (Wash. DC), *252:* 566–569, 1991.
39. Gondo, Y., Gardner, J. M., Nakatsu, Y., Durham-Pierre, D., Deveau, S. A., Kuper, C., and Brilliant, M. H. High-frequency genetic reversion mediated by a DNA duplication: the mouse pink-eyed unstable mutation. Proc. Natl. Acad. Sci. USA, *90:* 297–301, 1993.
40. Lyon, M. F., King, T. R., Gondo, Y., Gardner, J. M., Nakatsu, Y., Eicher, E. M., and Brilliant, M. H. Genetic and molecular analysis of recessive alleles at the pink-eyed dilution (*p*) locus of the mouse. Proc. Natl. Acad. Sci. USA, *89:* 6968–6972, 1992.
41. Schiestl, R. H., Aubrecht, J., Khogali, F., and Carls, N. Carcinogens induce reversion of the mouse pink-eyed unstable mutation. Proc. Natl. Acad. Sci. USA, *94:* 4576–4581, 1997.
42. Searle, A. G. The use of pigment loci for detecting reverse mutations in somatic cells of mice. Arch. Toxicol., *38:* 105–108, 1977.
43. Deol, M. S., and Truslove, G. M. The effects of the pink-eyed unstable gene on the retinal pigment epithelium of the mouse. J. Embryol. Exp. Morphol., *78:* 291–298, 1983.
44. Bodenstein, L., and Sidman, R. L. Growth and development of the mouse retinal pigment epithelium. II. Cell patterning in experimental chimaeras and mosaics. Dev. Biol., *121:* 205–219, 1987.
45. Bishop, A. J. R., Kosaras, B., Sidman, R. L., and Schiestl, R. H. Benzo(a)pyrene and X-rays induce reversions of the pink-eyed unstable mutation in the retinal pigment epithelium of mice. Mutat. Res, *457:* 31–40, 2000.
46. Schiestl, R. H., Khogali, F., and Carls, N. Reversion of the mouse pink-eyed unstable mutation induced by low doses of x-rays. Science (Wash. DC), *266:* 1573–1576, 1994.
47. Jalili, T., Murthy, G. G., and Schiestl, R. H. Cigarette smoke induces DNA deletions in the mouse embryo. Cancer Res., *58:* 2633–2638, 1998.
48. Lebel, M. Increased frequency of DNA deletions in pink-eyed unstable mice carrying a mutation in the Werner syndrome gene homologue. Carcinogenesis (Lond.), *23:* 213–216, 2002.
49. Aubrecht, J., Secretan, M. B., Bishop, A. J., and Schiestl, R. H. Involvement of p53 in X-ray induced intrachromosomal recombination in mice. Carcinogenesis (Lond.), *20:* 2229–2236, 1999.
50. Bertrand, P., Rouillard, D., Boulet, A., Levalois, C., Soussi, T., and Lopez, B. S. Increase of spontaneous intrachromosomal homologous recombination in mammalian cells expressing a mutant p53 protein. Oncogene, *14:* 1117–1122, 1997.
51. Mekeel, K. L., Tang, W., Kachnic, L. A., Luo, C. M., DeFrank, J. S., and Powell, S. N. Inactivation of p53 results in high rates of homologous recombination. Oncogene, *14:* 1847–1857, 1997.
52. Sturzbecher, H. W., Donzelmann, B., Henning, W., Knippschild, U., and Buchhop, S. p53 is linked directly to homologous recombination processes via RAD51/RecA protein interaction. EMBO J., *15:* 1992–2002, 1996.
53. Gebow, D., Miselis, N., and Liber, H. L. Homologous and nonhomologous recombination resulting in deletion: effects of p53 status, microhomology, and repetitive DNA length and orientation. Mol. Cell. Biol., *20:* 4028–4035, 2000.
54. Willers, H., McCarthy, E. E., Wu, B., Wunsch, H., Tang, W., Taghian, D. G., Xia, F., and Powell, S. N. Dissociation of p53-mediated suppression of homologous recombination from G_1/S cell cycle checkpoint control. Oncogene, *19:* 632–639, 2000.
55. Bodenstein, L., and Sidman, R. L. Growth and development of the mouse retinal pigment epithelium. I. Cell and tissue morphometrics and topography of mitotic activity. Dev. Biol., *121:* 192–204, 1987.
56. Bishop, A. J., Kosaras, B., Carls, N., Sidman, R. L., and Schiestl, R. H. Susceptibility of proliferating cells to benzo[a]pyrene-induced homologous recombination in mice. Carcinogenesis (Lond.), *22:* 641–649, 2001.
57. Sokal, R. R., and Rohlf, F. J. Biometrics, pp. 575–585. San Francisco: W. H. Freeman, 1969.
58. Wilcoxon, F. Individual comparisons by ranking methods. Biometrics, *1:* 80–83, 1945.
59. Mann, H. B., and Whitney, D. R. On a test of whether one of two random variables is stochastically larger than the other. Ann. Math. Stat., *18:* 50–60, 1947.
60. Nakayama, A., Nguyen, M. T., Chen, C. C., Opdecamp, K., Hodgkinson, C. A., and Arnheiter, H. Mutations in microphthalmia, the mouse homolog of the human deafness gene *MITF*, affect neuroepithelial and neural crest-derived melanocytes differently. Mech. Dev., *70:* 155–166, 1998.
61. MacCallum, D. E., Hupp, T. R., Midgley, C. A., Stuart, D., Campbell, S. J., Harper, A., Walsh, F. S., Wright, E. G., Balmain, A., Lane, D. P., and Hall, P. A. The p53 response to ionising radiation in adult and developing murine tissues. Oncogene, *13:* 2575–2587, 1996.
62. Gottlieb, E., Haffner, R., King, A., Asher, G., Gruss, P., Lonai, P., and Oren, M. Transgenic mouse model for studying the transcriptional activity of the p53 protein: age- and tissue-dependent changes in radiation-induced activation during embryogenesis. EMBO J., *16:* 1381–1390, 1997.
63. Komarova, E. A., Chernov, M. V., Franks, R., Wang, K., Armin, G., Zelnick, C. R., Chin, D. M., Bacus, S. S., Stark, G. R., and Gudkov, A. V. Transgenic mice with p53-responsive lacZ: p53 activity varies dramatically during normal development and determines radiation and drug sensitivity in vivo. EMBO J., *16:* 1391–1400, 1997.
64. Jones, S. N., Roe, A. E., Donehower, L. A., and Bradley, A. Rescue of embryonic lethality in Mdm2-deficient mice by absence of p53. Nature (Lond.), *378:* 206–208, 1995.
65. Montes de Oca Luna, R., Wagner, D. S., and Lozano, G. Rescue of early embryonic lethality in mdm2-deficient mice by deletion of p53. Nature (Lond.), *378:* 203–206, 1995.
66. Russell, L. B., and Russell, W. L. An analysis of the changing radiation response of the developing mouse embryo. J. Cell. Comp. Physiol., *43:* A103–A149, 1954.
67. Russell, L. B. Effects of low doses of x-rays on embryonic development in the mouse. Proc. Soc. Exp. Biol. Med., *95:* 174–178, 1957.
68. Allen, D. M., van Praag, H., Ray, J., Weaver, Z., Winrow, C. J., Carter, T. A., Braquet, R., Harrington, E., Ried, T., Brown, K. D., Gage, F. H., and Barlow, C. Ataxia telangiectasia mutated is essential during adult neurogenesis. Genes Dev., *15:* 554–566, 2001.
69. Xu, Y., Yang, E. M., Brugarolas, J., Jacks, T., and Baltimore, D. Involvement of p53 and p21 in cellular defects and tumorigenesis in Atm−/− mice. Mol. Cell. Biol., *18:* 4385–4390, 1998.
70. Xu, Y., Ashley, T., Brainerd, E. E., Bronson, R. T., Meyn, M. S., and Baltimore, D. Targeted disruption of ATM leads to growth retardation, chromosomal fragmentation during meiosis, immune defects, and thymic lymphoma. Genes Dev., *10:* 2411–2422, 1996.
71. Donehower, L. A., Harvey, M., Slagle, B. L., McArthur, M. J., Montgomery, C. A., Jr., Butel, J. S., and Bradley, A. Mice deficient for p53 are developmentally normal but susceptible to spontaneous tumours. Nature (Lond.), *356:* 215–221, 1992.
72. Jacks, T., Remington, L., Williams, B. O., Schmitt, E. M., Halachmi, S., Bronson, R. T., and Weinberg, R. A. Tumor spectrum analysis in p53-mutant mice. Curr. Biol., *4:* 1–7, 1994.